Supplementary Materials: The "Carbonaceous aerosol in Rome and Environs (CARE)" project: first results

Francesca Costabile [1]*,Honey Alas [2], Michaela Aufderheide[3], Pasquale Avino [4], Fulvio Amato [5], Stefania Argentini [1], Francesca Barnaba [1], Massimo Berico [6], Vera Bernardoni [7], Riccardo Biondi [1], Giulia Calzolai [8], Silvia Canepari [9], Giampietro Casasanta [1], Spartaco Ciampichetti [1], Alessandro Conidi [1], Eugenia Cordelli [10], Antonio Di Ianni [1,11], Luca Di Liberto [1], Maria Cristina Facchini [1], Andrea Facci [11], Daniele Frasca [9], Stefania Gilardoni [1], Maria Giuseppa Grollino [6], Maurizio Gualtieri [6], Franco Lucarelli [8], Antonella Malaguti [6], Maurizio Manigrasso [4], Mauro Montagnoli [12], Silvia Nava [8], Elio Padoan [5,13], Cinzia Perrino [12], Ettore Petralia [6], Igor Petenko [1] , Xavier Querol [5], Giulia Simonetti [9], Giovanna Tranfo [4], Stefano Ubertini [11], Gianluigi Valli [7], Sara Valentini [7], Roberta Vecchi [7], Francesca Volpi [1], Kay Weinhold [2], Alfred Wiedensholer [2], Gabriele Zanini [6] and Gian Paolo Gobbi [1]

This document presents supplementary materials for the article "The Carbonaceous aerosol in Rome and Environs (CARE) project: first results"

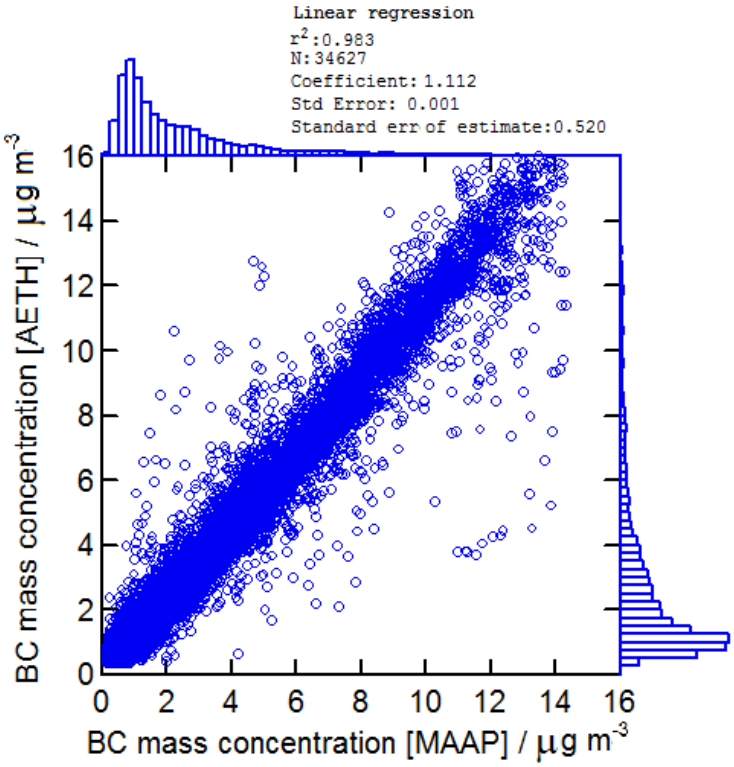

Figure S1. Scatter plot of 1-minute eBC mass concentration from MAAP versus 1-minute eBC mass concentration from AE-33 aethalometer. Relevant linear regression variables are indicated. Data are presented with histograms of the probability distribution function.

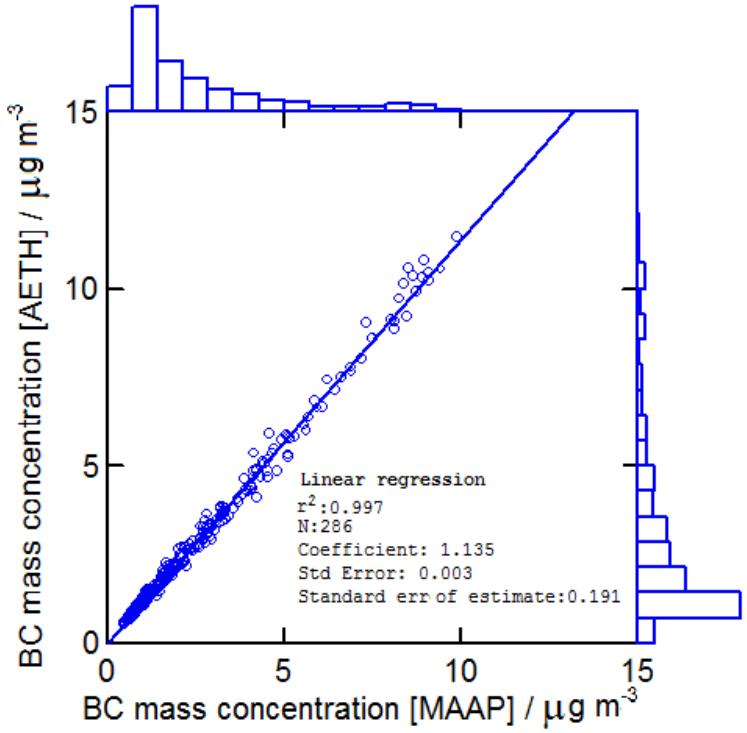

Figure S2. Scatter plot of 2-hour averaged eBC mass concentration from MAAP versus 2-hour averaged eBC mass concentration from AE-33 aethalometer. Relevant linear regression variables are indicated. Data are presented with histograms of the probability distribution function.

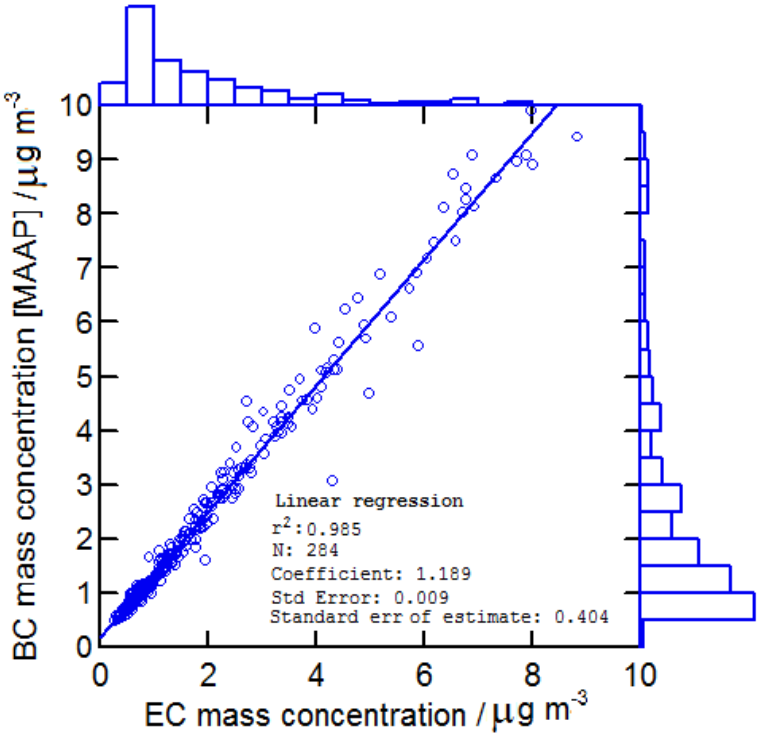

Figure S3. Scatter plot of 2-hour averaged eBC mass concentration from MAAP versus EC mass concentration from 2h Sunset. Relevant linear regression variables are indicated. Data are presented with histograms of the probability distribution function.

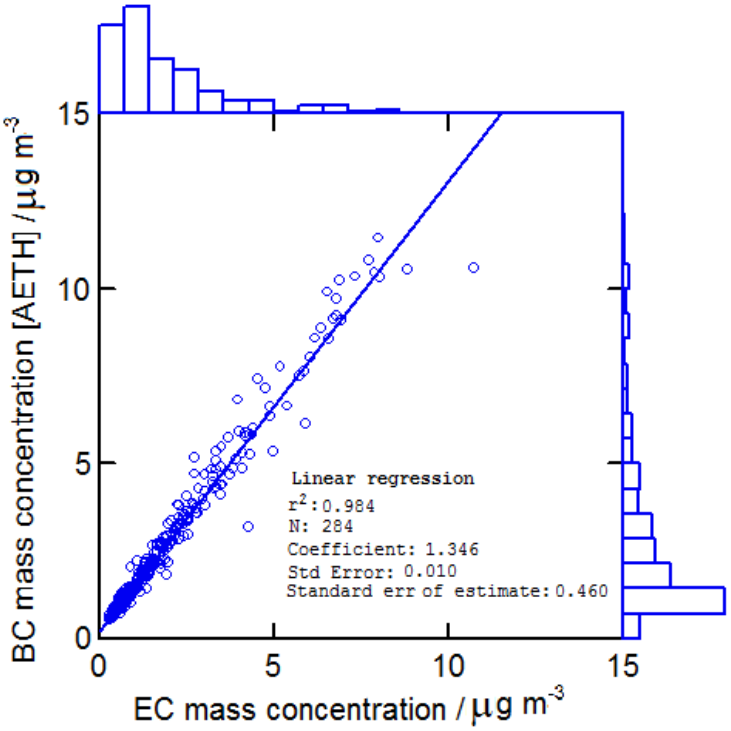

Figure S4. Scatter plot of 2-hour averaged BC mass concentration from AE-33 aethalometer versus EC mass concentration from 2h Sunset. Relevant linear regression variables are indicated. Data are presented with histograms of the probability distribution function.

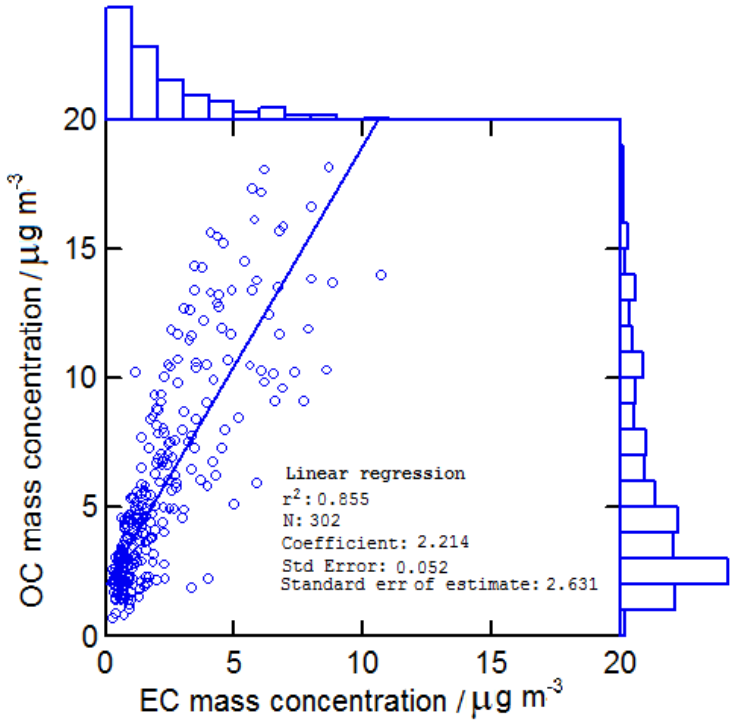

Figure S5. Scatter plot of OC vs EC mass concentrations from 2h Sunset. Data are presented with relevant histograms of the probability distribution function.

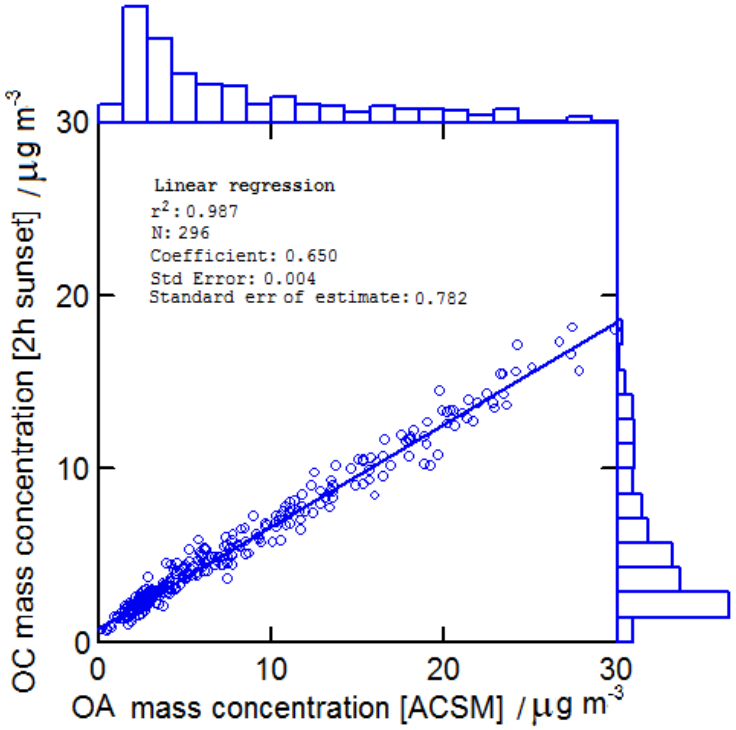

Figure S6. Scatter plot of OC mass concentrations from 2h Sunset vs OM mass concentration from ACSM. Data are presented with relevant histograms of the probability distribution function.

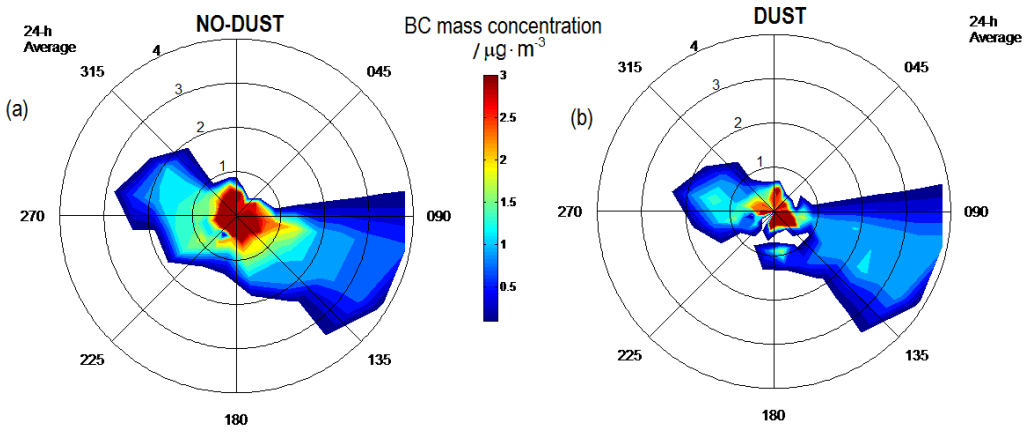

Figure S7. Wind rose under no-dust and dust conditions.

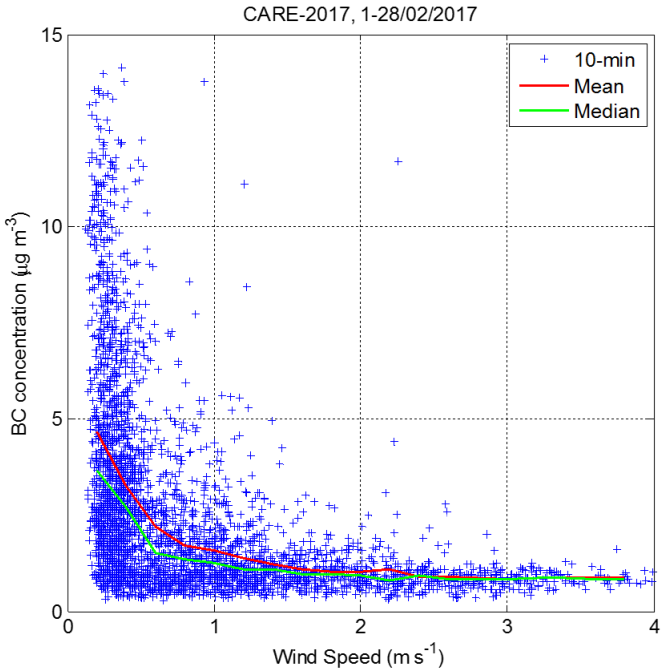

Figure S8. Scatterplot of the BC concentration versus wind speed.

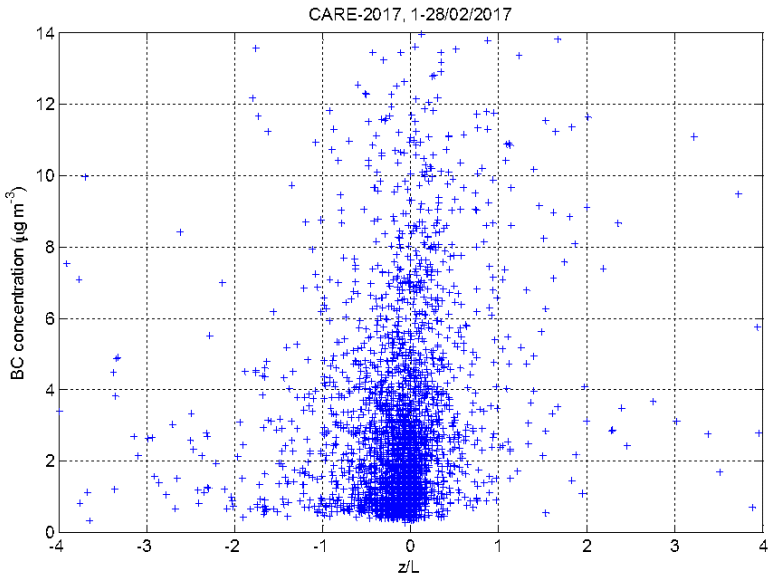

Figure S9. Scatter plot of the black carbon concentration versus the inverse of Monin Obukov length (z/L).

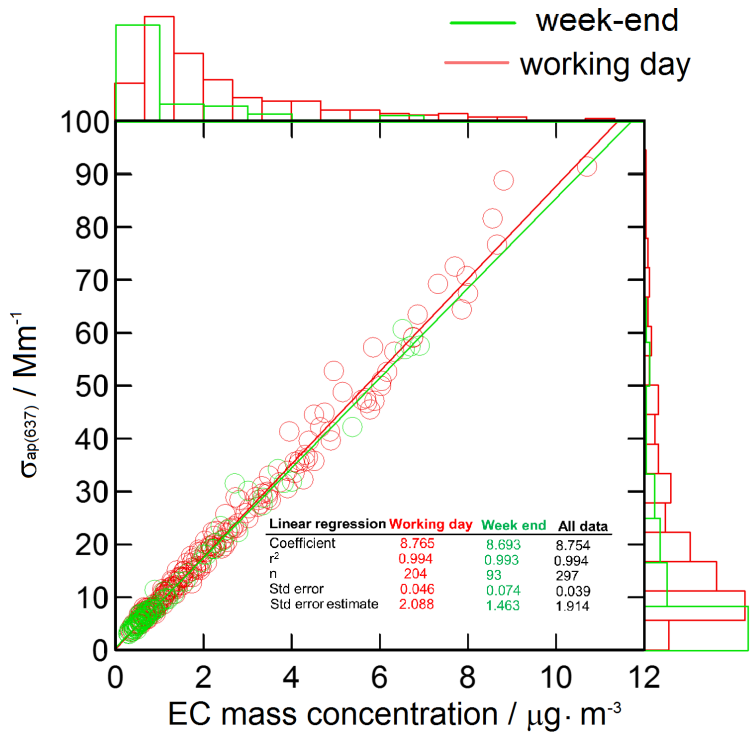

Figure S10. Mass Absorption Coefficient at 637 nm (MAC637) calculated as regression analysis of the absorption coefficient at 637 nm from MAAP and EC mass concentrations from Sunset. Data are presented with relevant histograms of the probability distribution function .

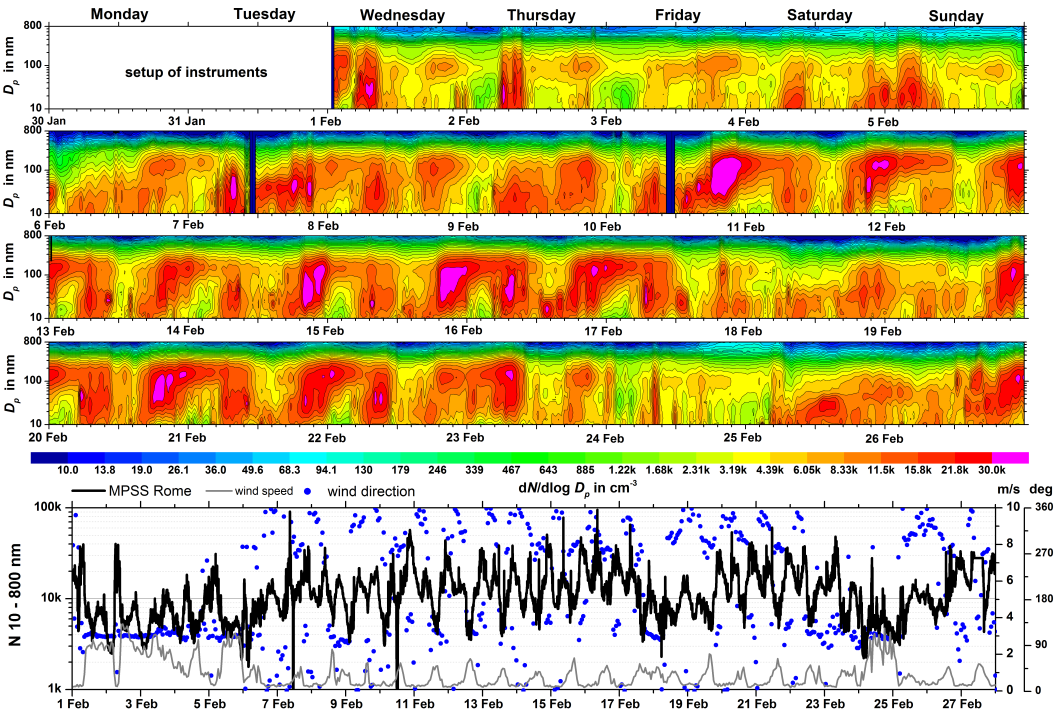

Figure S11. Particle number size distribution from 8 to 800 nm measured during the campaign.

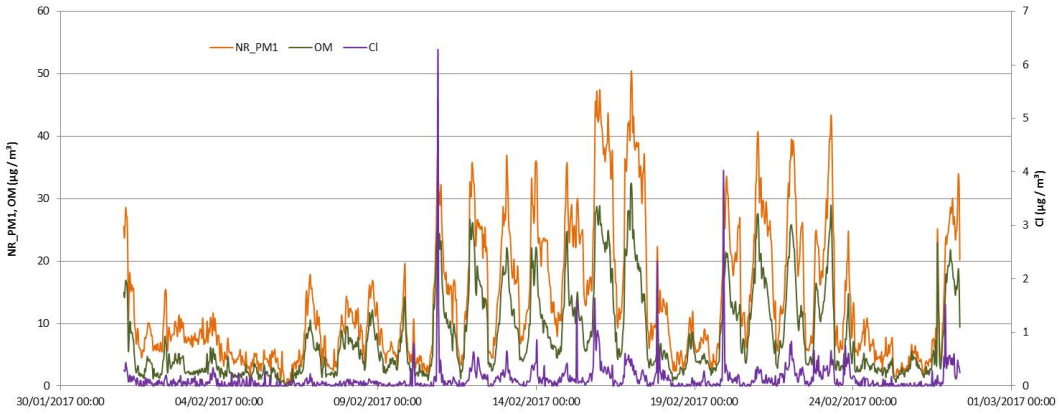

Figure S12. Time series of total NR-PM_1 and of the organics and chloride within the NR-PM_1 as measured by the ACSM.

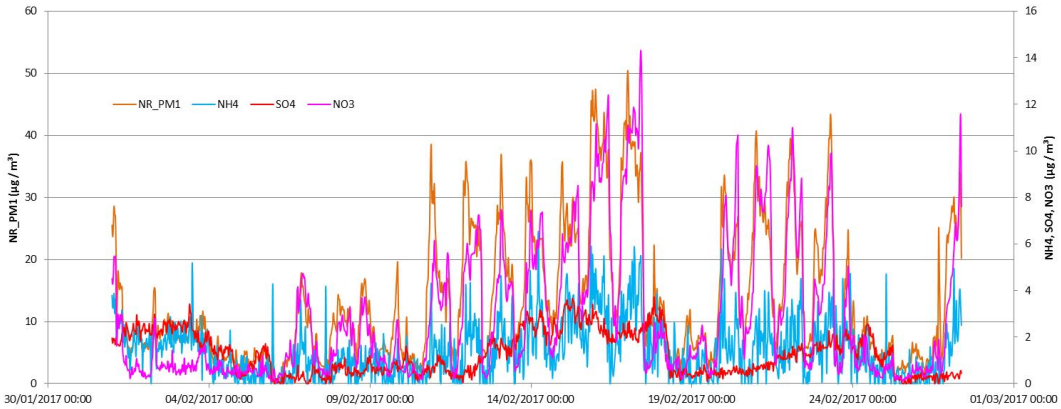

Figure S13. Time series of total NR-PM_1 and of the ammonium, sulfate, nitrate within the NR-PM_1 as measured by the ACSM.

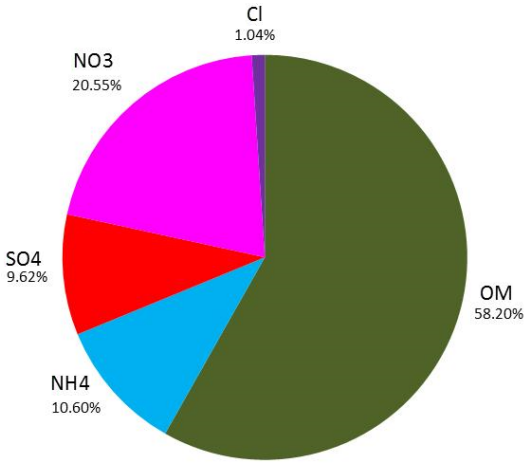

Figure S14. Percent contributions of the organics, ammonium, sulfate, nitrate, and chloride to the total NR-PM_1 as measured by the ACSM.

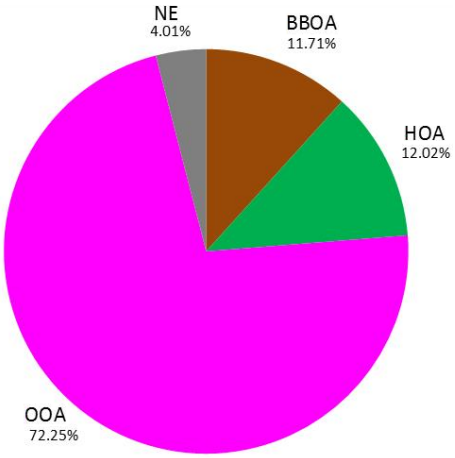

Figure S15. Percentage contributions of Vehicular traffic emission (HOA), Biomass burning emission (BBOA) and Oxidized organic aerosol (OOA) to the total NR-PM_1 organic aerosol concentration.

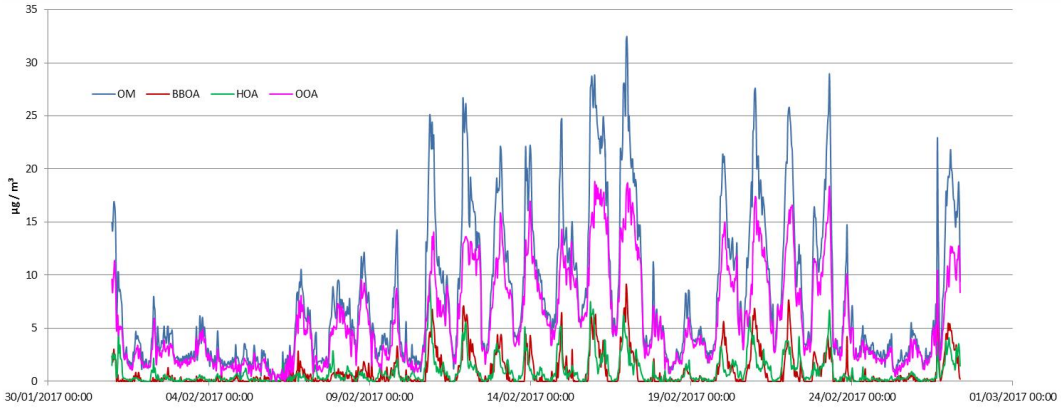

Figure S16. Temporal variability (time resolution 30 min) of the whole OA and of the three factors (BBOA, HOA, OOA).

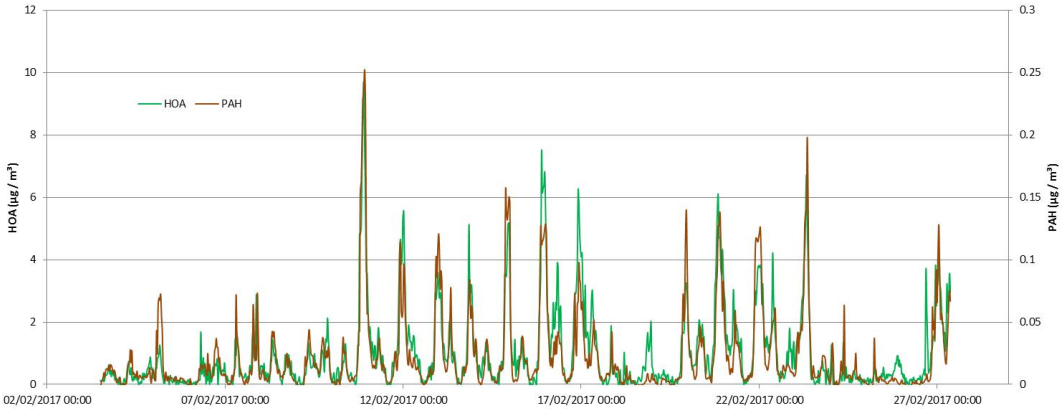

Figure S17. Temporal variability (time resolution 30 min) of HOA and total PAHs.

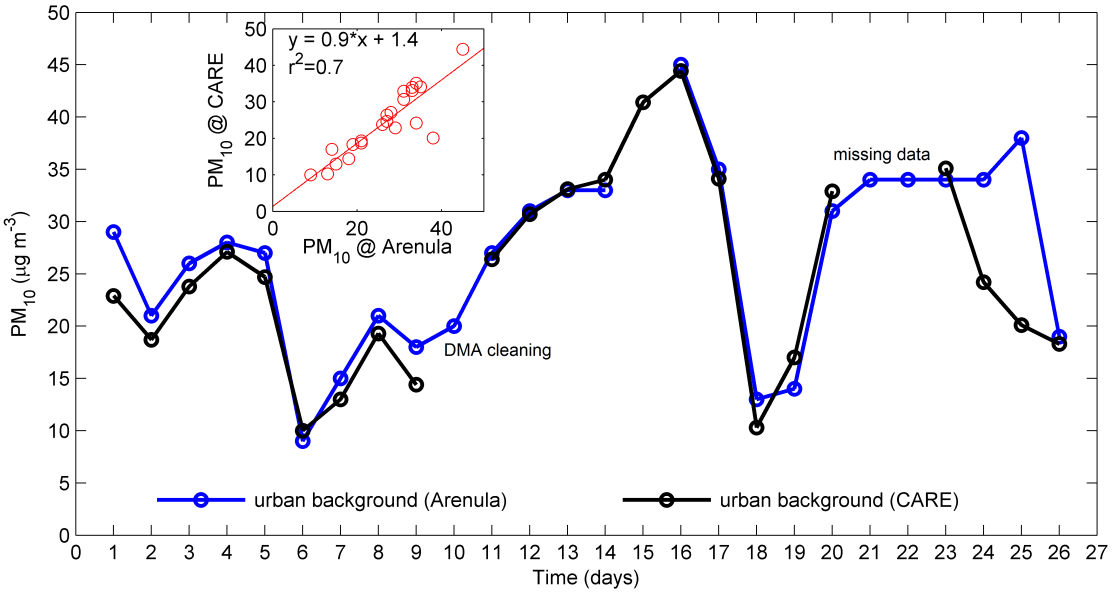

Figure S18. Temporal variations of 24-h PM_{10} reconstructed from aerosol size distribution data (SMPS+APS) at the CARE site. Data are compared to 24-h PM_{10} values measured by the local environmental agency (ARPA Lazio) at the closest urban background station (Arenula, 3 km from the CARE site).

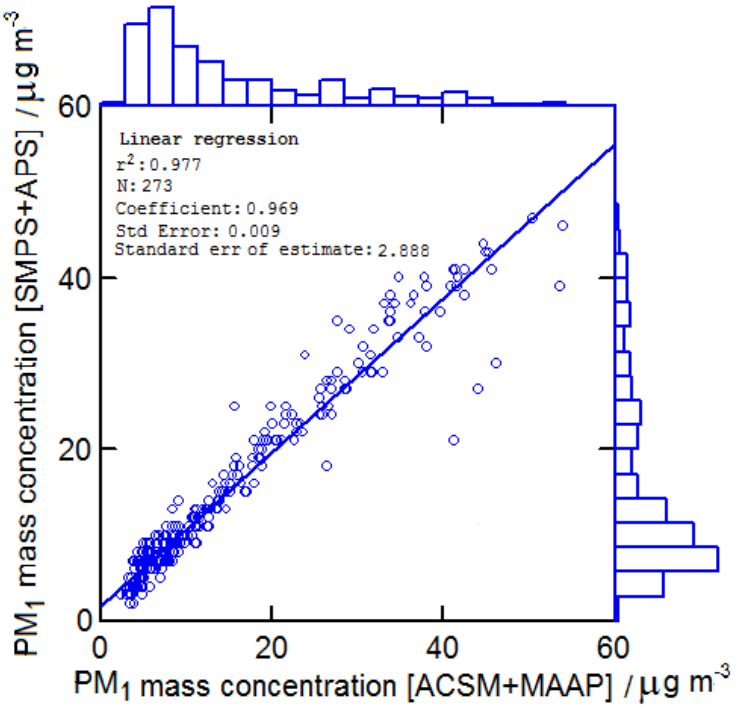

Figure S19. Scatter plot of PM_1 mass concentration from NR-PM_1 mass concentration measured by ACSM and eBC mass concentration measured by MAAP versus PM_1 mass concentration reconstructed from particle size distribution data measured from SMPS and APS. Relevant linear regression variables are indicated. Data are presented with histograms of the probability distribution function.

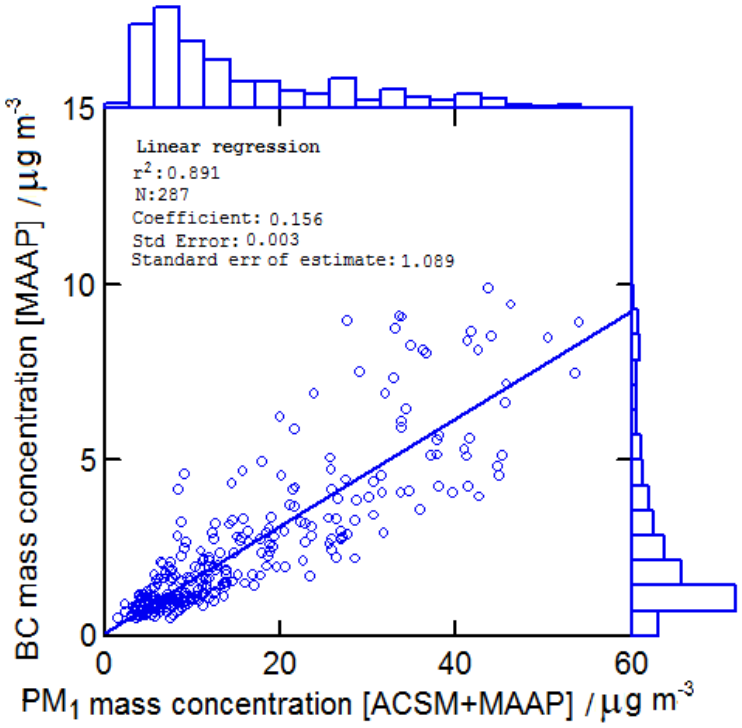

Figure S20. Scatter plot of eBC mass concentration measured by MAAP versus PM_1 mass concentration reconstructed from ACSM and MAAP. Relevant linear regression variables are indicated. Data are presented with histograms of the probability distribution function.

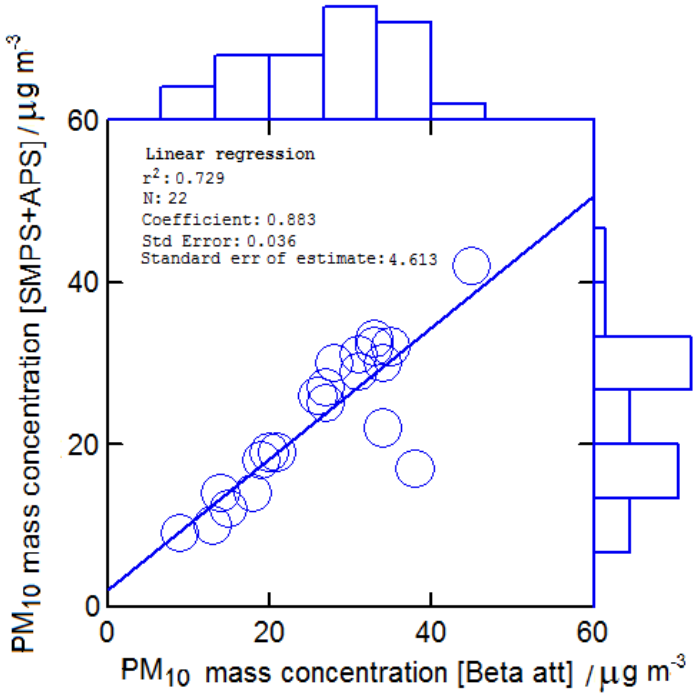

Figure S21. Scatter plot of PM_{10} mass concentration from analyser based on beta attenuation monitor versus PM_{10} mass concentration reconstructed from particle size distribution data measured from SMPS and APS. Relevant linear regression variables are indicated. Data are presented with histograms of the probability distribution function.

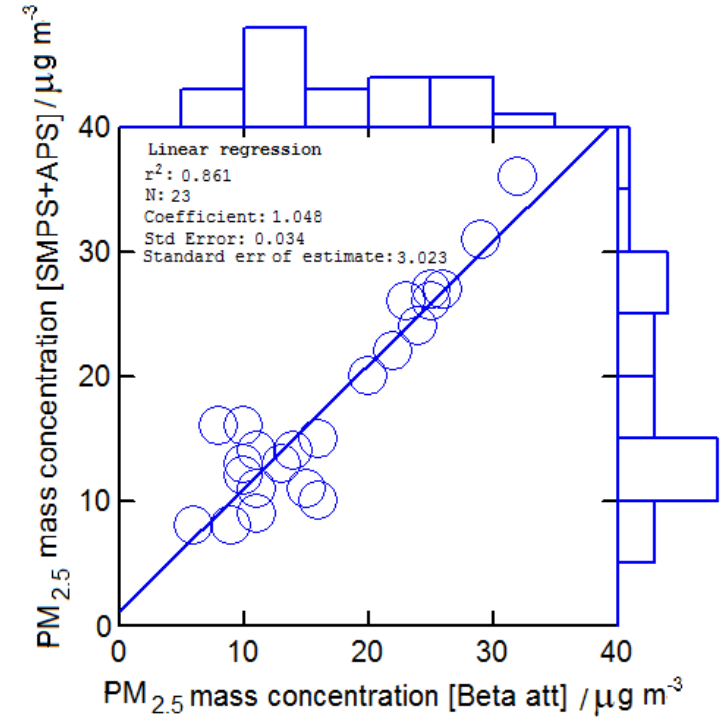

Figure S22. Scatter plot of $PM_{2.5}$ mass concentration from analyser based on beta attenuation monitor versus $PM_{2.5}$ mass concentration reconstructed from particle size distribution data measured from SMPS and APS. Relevant linear regression variables are indicated. Data are presented with histograms of the probability distribution function.

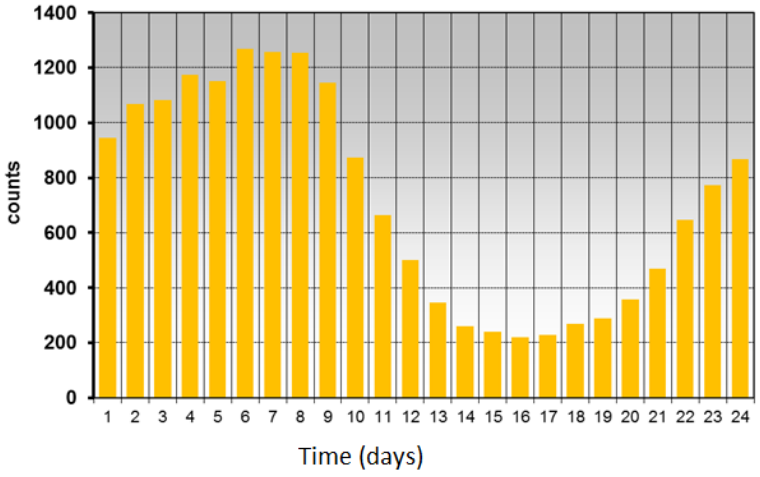

Figure S23. Mean diurnal cycle of natural radioactivity.

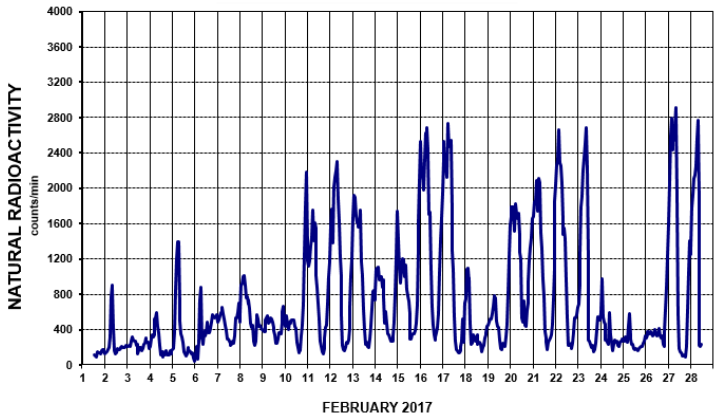

Figure S24. Time series of natural radioactivity.

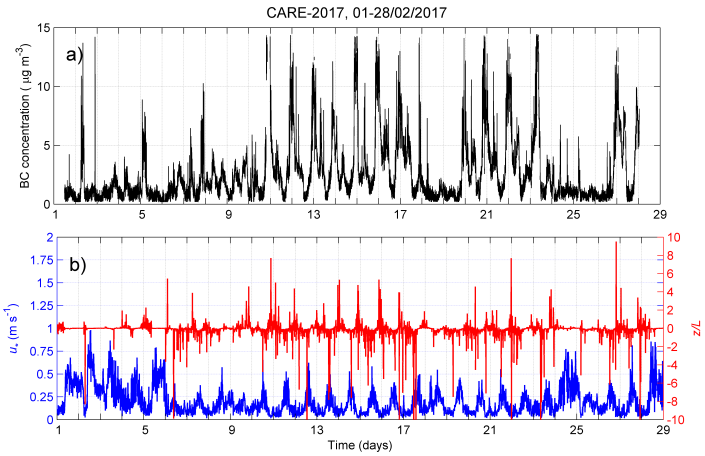

Figure S25. Time series of the eBC mass concentration and Monin - Obukov length (z/L).

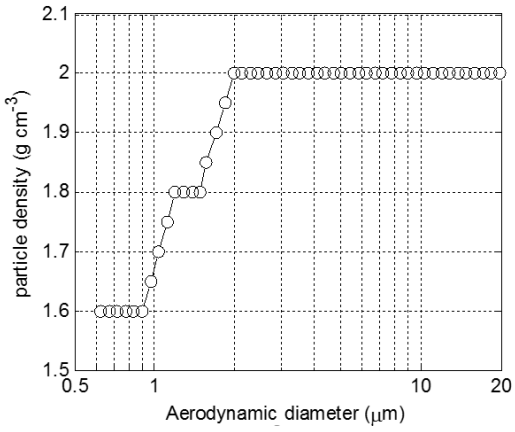

Figure S26. Particle density used to convert APS data.

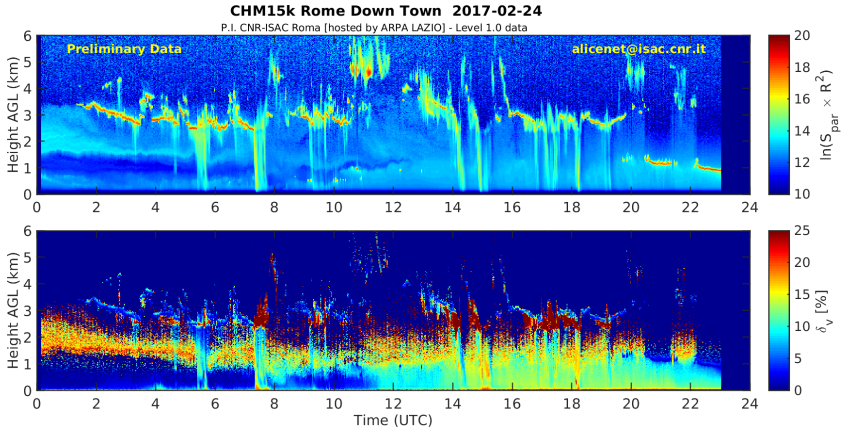

Figure S27. The Polarisation Lidar Ceilometer plots of February 24, 2017. The upper plot shows the range-corrected backscatter signal intensity. The (%) depolarization signal reported in the lower panel shows the presence of the dust layer between 1.5 and 2.5 km altitude in the morning. This layer then descends to the ground in the afternoon. Precipitation is also observed to convey dust towards the ground along several showers between 5.30 and 7pm (UTC).

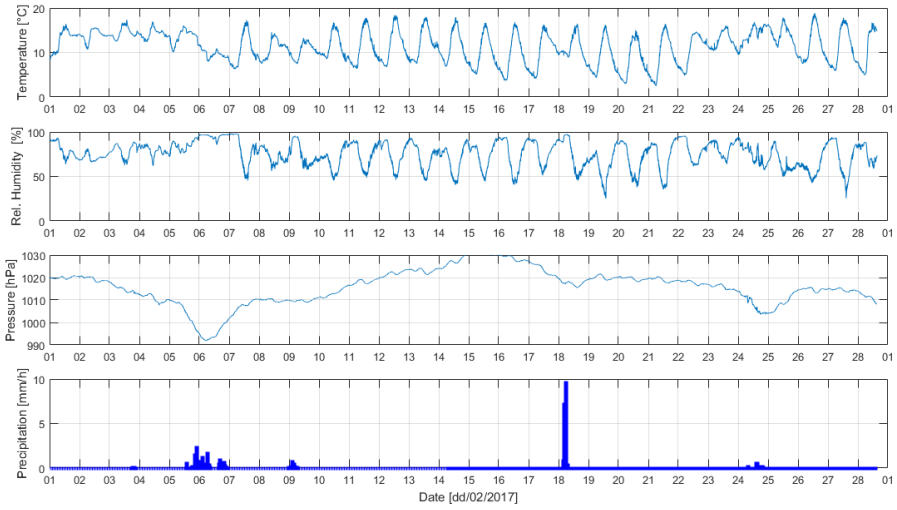

Figure S28. Time series of Temperature, relative humidity, pressure and precipitation measured at the S.Sito site during the CARE experiment.